# APPLYING LUMINESCENT OXYGEN SENSORS IN HYDROGELS

by
Cheng Yang

A thesis submitted to Johns Hopkins University in conformity with the requirements for

the degree of Master of Science in Engineering

Baltimore, Maryland
May 2021

# Abstract

Oxygen is important for maintaining daily activities of all living creatures and monitoring oxygen concentration has great significance in biomedical fields. Luminescent oxygen sensors have attracted scientists' attention for their high accuracy, resistance to interference, and the ability to achieve continuous non-invasive monitoring of oxygen levels *in vivo* and *in vitro*. Platinum porphyrin compound platinum(II)-5,10,15,20-tetrakis-(2,3,4,5,6-pentafluorophenyl)-porphyrin (PtTFPP) is an oxygen sensing probe with high sensitivity, high quantum yield and long luminescence lifetime. However, its hydrophobicity limits its application in biological studies. To overcome its hydrophobicity, we synthesized amphiphilic block copolymers poly(ε-caprolactone)-block-poly(hydroxypropyl methacrylamide) (PCL-b-PHPMA) with both a hydrophobic segment PCL and a hydrophilic segment PHPMA to encapsulate hydrophobic PtTFPP. The polymers can self-assemble into micelles in water, and PtTFPP could be used as oxygen sensors in water solutions, with which cells and tissues are compatible. We tested the sensors in collagen I hydrogels, which can structurally and biomechanically mimic extracellular matrix (ECM), with and without oxygen-consuming KIA cells in the hydrogels to provide a hypoxic environment for oxygen sensors to show oxygen distribution. The polymeric oxygen sensor showed good oxygen sensing properties in micelle solutions and hydrogels based on its phosphorescence under certain excitations.

**Primary Reader and Advisor:** Dr. Sharon Gerecht

# Acknowledgement

I would like to express my greatest appreciation to my supervisor Dr. Sharon Gerecht for her valuable and constructive suggestions during the establishment and development of this research work. Dr. Sharon Gerecht has given me so much useful guidance in the field of materials science and chemical biomolecular engineering. Her guidance and encouragement are very important to me and makes me always enthusiastic for science and research. Without her kindness and generous help this thesis would not have been possible.

I would like to offer my special thanks to my mentor Ms. YingYu Lin for her help, patience and encouragement. She has helped me getting familiar with our lab at the very beginning and guided me throughout the whole project. Ms. YingYu Lin is so warmhearted and generous that I would like to thank her from the bottom of my heart.

I wish to acknowledge the help provided by Dr. Rachel Latanich, Ms. Christine Duke, Dr. Morgan Elliott, Ms. Eugenia Volkova, Ms. Jane Nguyen, Ms. Sydney Conner, Mr. Dimitris Ntekoumes and all our lab members. Everyone in our lab is so kind and helpful and I really appreciate the time we spent together.

Assistance provided by Dr. Wang lab, Dr. Mao lab, Dr. Tsapatsis lab, Dr. Katz lab, NMR Core Facility in Department of Chemistry, Integrated Imaging Center and Institute of Nanobiotechnology in JHU are greatly appreciated.

I would also like to extend my thanks to Ms. Yiyan Lin, Ms. Mingli Gong, Ms. Chenxi Liu, Ms. Chang Liu and Mr. Yuanxin Qiu for their support and company during my hard time.

# Dedication

This thesis is dedicated to my beloved parents, Limao Yang and Yinghui Dong, for their encouragement, tolerance, support, trust and love throughout my life.

# Contents

# List of Figures

# 1. Introduction

Oxygen is one of the most important elements on earth, it is essential for the maintenance of human, animal and plant life activities. For animals, oxygen is the source of generating energy needed to maintain normal physiological functions. Increase or decrease of oxygen concentration will influence the normal physiological function of organisms[1, 2], therefore the monitoring of oxygen concentration has important significance in the field of biomedical studies. For example, hypoxia-inducible factors (HIFs) can accumulate under hypoxic microenvironments (where oxygen concentration is lower than 5%) and can regulate cell behaviors and functions[3, 4], and here measuring oxygen concentration becomes highly important to monitor hypoxia.

Dissolved oxygen is the amount of gaseous oxygen that is dissolved in solvents[5]. Methods for monitoring dissolved oxygen concentration include chemical analysis method[6], electrochemical method[7], and optical analysis method[8, 9]. Chemical analysis method uses iodine generated during the titration of sodium to measure dissolved oxygen concentration[6]. While chemical analysis is accurate, it is not suitable for continuous and real-time oxygen concentration monitoring. Electrochemical method measures dissolved oxygen concentration indirectly by measuring the current generated on the electrode in low oxygen environment[7]. This method is highly sensitive and rapid but requires a needle-like probe for the measurement, which is invasive and can damage the sample. Optical analysis method uses luminescent metal-complexes nanoprobes to measure oxygen concentrations[9]. Quenching occurs when luminescent probe molecules are in excited states and oxygen molecules are in ground states[10, 11]. During quenching, the energy

gained by luminescent molecules during excitation can be transferred to oxygen molecules. Since the concentration of dissolved oxygen is usually much lower than the concentration of luminescent molecules, only a small portion of energy can be transferred to oxygen molecules. The rest of the energy dissipates from the luminescent molecules in the form of phosphorescence. After emission of phosphorescence, the luminescent molecules return to ground states. The phosphorescent signal was collected by a spectrometer or a microscope and used for calculating oxygen concentration. Phosphorescence intensity of a luminescent molecule changes with the oxygen concentration. The relationship between luminescent intensity and oxygen concentration can be calculated by the Stern-Volmer equation shown below[12]:

$$\frac{I}{I_0} = 1 + K_{SV} \cdot [\mathrm{O_2}]$$

Here, $I$ is phosphorescence intensity, $I_0$ is phosphorescence intensity of luminescent molecules in the deoxygenated environment, $[O_2]$ is oxygen concentration, and $K_{SV}$ is Stern-Volmer quenching constant. This oxygen measurement method is accurate, resistant to interference, and is able to achieve continuous non-invasive monitoring[13].

Pt(II) porphyrin compound, platinum(II)-5,10,15,20-tetrakis-(2,3,4,5,6-pentafluorophenyl)-porphyrin (PtTFPP) is an optical oxygen nanoprobe[14, 15]. Porphyrin compounds have great absorption in visible spectra, long luminescence lifetime (tens of microseconds), large Stokes shift and high rate of oxygen quenching[16, 17]. However, PtTFPP is not soluble in water which hindered its usage in biological fields.

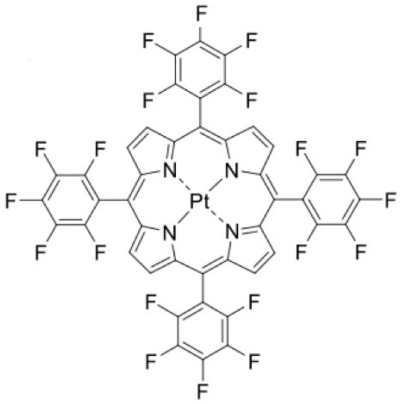


Figure 1. Structure of PtTFPP

Amphiphilic block copolymers poly( $\varepsilon$ -caprolactone)-*block*-poly(hydroxypropyl methacrylamide) (PCL-*b*-PHPMA) were adopted to encapsulate hydrophobic PtTFPP. PCL-*b*-PHPMA can self-assemble into micelles in water due to its hydrophobic segment PCL and hydrophilic segment PHPMA[18, 19]. Once dissolved in water, the hydrophilic segment PHPMA will form a shell structure in contact with water, while the hydrophobic segment PCL along with PtTFPP will form a core structure inside the shell. PtTFPP encapsulated in the micelles can be used as oxygen sensors to measure oxygen concentration in water solutions[20]. We also adopted collagen I hydrogels, which can act functionally similar as extracellular matrix (ECM)[21, 22], and embedded oxygen-consuming KIA cells in the hydrogels to provide a hypoxic environment for oxygen sensors to show oxygen distribution.

# 2. Experimental Section

## 2.1 Materials

$\varepsilon$-Caprolactone ($\varepsilon$-CL, ≥98%), tin(II) 2-ethylhexanoate ($Sn(Oct)_2$, 95%), benzyl alcohol (anhydrous, 99.8%), 4-cyano-4-(phenylcarbonothioylthio) pentanoic acid (CTA, 99.9%), N,N'-dicyclohexylcarbodiimide (DCC, 99%), 2,2′-azobis(2-methylpropionitrile) (AIBN, 98%), toluene (anhydrous, 99.8%), methanol (anhydrous, 99.8%), diethyl ether (anhydrous, ≥ 99.7%), 4-(dimethylamino)pyridine (DMAP, ≥ 99%), N,N-dimethylformamide (DMF, anhydrous, 99.8%), dichloromethane (DCM, anhydrous, ≥99.8%), and dimethyl sulfoxide (DMSO, anhydrous, ≥99.9%) were purchased from Sigma Aldrich (St. Louis, MO) and used as received. 2-Hydroxypropyl methacrylamide (HPMA, 99%) was purchased from AK Scientific (Union, CA). Pt(II) meso-tetra(pentafluorophenyl)porphine (PtTFPP) was purchased from Frontier Scientific (Logan, Utah). Collagen I was purchased from Corning (Glendale, AZ).

## 2.2 Instruments

UV-vis spectra and fluorescence spectra were recorded using a SpectraMax M3 microplate reader (Molecular Devices, San Jose,CA). Lyophilization was performed by a FreeZone 2.5 L Lyophilizer (Labconco, Kansas, MO). Dynamic light scattering (DLS) measurements were done by Zetasizer Nano systems (Malvern Panalytical, Westborough, MA). 0.45 $\mu$m PTFE syringe filters were purchased from CellTreat Scientific (Pepperell, MA). Nuclear magnetic resonance (NMR) spectra were obtained by a Bruker Avance 300 MHz spectrometer. Milli-Q water was provided by Milli-Q reference

water purification system (Millipore, Darmstadt, Germany). Confocal images were taken by a Zeiss LSM 780 confocal microscope (Zeiss, Germany).

## 2.3 Synthesis of PCL

0.1045 g benzyl alcohol (0.966 mmol), 5.029 g $\varepsilon$-CL (0.044 mol), 0.125 g $Sn(Oct)_2$ (0.309 mmol) and 10 mL of toluene were mixed in a 50 mL Schlenk flask. Due to the low boiling point of toluene (approximately at 110 $^oC$), a reflux condenser was used on the top ground joint of the flask. The top of the reflux condenser was capped with a rubber septum and sealed with Parafilm. The side-arm of the flask was connected to a cold trap through tubing then the cold trap was connected to vacuum source. Both the flask and the cold trap were immersed in liquid nitrogen during air-removing process. The mixture was degassed three times through a freeze-pump-thaw cycle. After removing air from the flask, the flask was refilled with gaseous nitrogen and the side-arm of the flask was connected to an oil bubbler. The flask was immersed in an oil bath and the reflux condenser was connected to continuous flushing cold water. Reaction was conducted at 110 $^oC$ for 24 hours. 24 hours later, the reaction was terminated by being cooled down rapidly in an ice bath. The reaction mixture was diluted with 15 mL of DCM and the product was precipitated by dropwise adding the mixture into 200 mL of cold methanol under vigorous stirring. The precipitation was filtered using Buchner funnel and washed with another 150 mL of cold methanol. The product PCL was dried under reduced pressure in a vacuum oven.

## 2.4 Modifying PCL With Chain Transfer Agent

0.1 g DCC (0.485 mmol) was weighed into a glass vial and sealed with Parafilm in glovebox. 0.5 g PCL, 0.1 g CTA (0.358 mmol), 0.012 g DMAP (0.0968 mmol) and 5 mL of DCM were mixed in a 20 mL Schlenk flask. The top ground joint of the flask was tightly capped with a rubber septum and sealed with Parafilm. The side-arm of the flask was connected to a cold trap through tubing and the cold trap was connected to vacuum source. Both the flask and the cold trap were immersed in liquid nitrogen during air-removing process. The mixture was degassed three times through a freeze-pump-thaw cycle. After removing air from the flask, the flask was refilled with gaseous nitrogen. The mixture was cooled down to 0 $^{o}$C in an ice bath. 0.1 g DCC was dissolved in 3 mL of DCM and dropwise removed from glass vial to the flask. The reaction was conducted at room temperature for 24 hours in the dark. The reaction was terminated after 24 hours, the byproduct dicyclohexylurea was removed by filtration. The product was precipitated by dropwise adding the mixture into 350 mL of cold methanol under vigorous stirring. The precipitation was filtered using Buchner funnel and the product PCL-CTA was dried under reduced pressure in a vacuum oven.

## 2.5 Synthesis of Amphiphilic PCL-*b*-PHPMA Diblock Copolymer

0.400 g HPMA (2.794 mmol) and 0.001 g AIBN (0.006 mmol) were weighed into separate glass vials and sealed with Parafilm in glovebox. 0.100 g PCL-CTA, 0.400 g HPMA, 0.001 g AIBN and 5 mL DMF was mixed in a 20 mL Schlenk flask. The top ground joint of the flask was tightly capped with a rubber septum and sealed with Parafilm. The side-arm of the flask was connected to a cold trap through tubing and the cold trap was connected to vacuum source. Both the flask and the cold trap were immersed in liquid nitrogen during air-removing process. The mixture was degassed six times through a

freeze-pump-thaw cycle. After removing air from the flask, the flask was refilled with gaseous nitrogen. The reaction was conducted at 70 $^{o}$C for 24 hours. The reaction was terminated by being cooled down rapidly in an ice bath. The product was precipitated by dropwise adding the mixture into 200 mL of cold diethyl ether under vigorous stirring. The precipitation was filtered using Buchner funnel and washed with 100 mL of cold diethyl ether for three times. The product PCL-b-PHPMA was dried under reduced pressure in a vacuum oven.

## 2.6 Characterization of PCL, PCL-CTA and PCL-*b*-PHPMA

$^{1}$H NMR spectra were used to characterize the structures of polymers and their molecular weights can therefore be calculated. 7 mg PCL and 6 mg PCL-CTA were dissolved in 0.6 mL of $CDCl_3$ separately, and 3 mg PCL-*b*-PHPMA was dissolved in 0.6 mL of DMSO-$d_6$ in NMR tubes at room temperature overnight before measurement. The spectra were measured at room temperature and analyzed using TopSpin.

## 2.7 Preparation of Micelles

2 mg PtTFPP was dissolved in 1 mL of DMSO overnight and 25 mg amphiphilic copolymer PCL-*b*-PHPMA was then added in the mixture. The mixture was slowly injected into 6 mL of Milli-Q water under vigorous stirring to form micelles. The micelle solution was transferred into a dialysis bag with molecular weight cut off at 3500, and was dialyzed in DI water for 3 days, with water changed every 12 hours to remove DMSO. After dialysis, the micelle solution was filtered through a 0.45 $\mu$m syringe filter to remove non-incorporated PtTFPP and precipitated polymers. The micelle solutions were being stored at 4 $^{o}$C.

## 2.8 Calibration of Micelles

The average particle size of the micelle solution was characterized by DLS at room temperature for three times. To determine the concentrations of PtTFPP and PCL-*b*-PHPMA in micelle solution, 1 mL of micelle solution was lyophilized to obtain solid-state PCL-*b*-PHPMA and PtTFPP. The lyophilized product was re-dissolved in 1 mL mixture of DMSO and water (90:10 by volume). A standard curve of absorption of PtTFPP at 390 nm was obtained using a 96 well plate and a microplate reader. The concentration of PtTFPP in lyophilized solution can be calculated. By comparing to the weight of lyophilized product, the concentration of PCL-*b*-PHPMA can therefore be determined.

## 2.9 Oxygen Sensing Performances of Sensors in Micelle Solutions

To test the oxygen sensing ability of the micelle solution, the phosphorescence spectra of hypoxic (approximately 0% of dissolved oxygen) and normoxic (approximately 21% of dissolved oxygen, in a concentration of 8 mg/mL) 10-times diluted micelle solutions were recorded with excitation wavelength at 390 nm using a 96 well plate and a microplate reader. To fully remove dissolved oxygen from micelle solution, gaseous nitrogen flowed into micelle solution for three minutes. 500-750 nm Emission spectra were recorded at the excitation wavelength of 390 nm. All measurements were done at room temperature and atmosphere pressure.

## 2.10 Oxygen Sensing Performances of Sensors in Collagen Hydrogels

The 7.1 mg/mL collagen I diluted stock was prepared in 0.1% acetic acid and stored at 4 $^{o}$C. To consume oxygen, simian T-cell lymphotropic virus (STLV) infected baboon T-cell line (KIA) was used.

For collagen hydrogel with KIA cells, 7.21 $\mu$L of M199(10X), 20 $\mu$L of micelle solution, 64.68 $\mu$L of collagen I and 1.94 $\mu$L of 1M NaOH was added to one Eppendorf tube and mixed quickly until uniform. 369600 of KIA cells were suspended in 74.03 $\mu$L of M199(1X) and added into the tube. The mixture was mixed well quickly and 60 $\mu$L of mixture was added to each well of a 96 well plate.

For collagen hydrogel without cells, 7.21 $\mu$L of M199(10X), 20 $\mu$L of micelle solution, 64.68 $\mu$L of collagen I and 1 $\mu$L of 1M NaOH was added to one Eppendorf tube and mixed quickly until uniform. 56 $\mu$L of mixture was added to each well of a 96 well plate.

All hydrogels were incubated at 37 $^{o}$C for 30 minutes. Then 200 $\mu$L of DMEM (Dulbecco's modified Eagle's medium) was added onto each well. The samples were taken images after 24 hours of incubation using a Zeiss LSM 780 confocal microscope at the excitation wavelength of 405 nm and at the emission wavelength of 640 nm.

# 3. Results and Discussion

## 3.1 Polymer Synthesis and Characterization

The synthesis of amphiphilic block copolymers is shown in Scheme 1. PCL was synthesized by a ring-opening polymerization from monomer caprolactone, where benzyl alcohol was used as initiator and $Sn(Oct)_2$ was used as catalyst. The molecular weight of PCL was 2.86 kDa and the repeating number *x* was 23 determined by $^1H$ NMR. This was calculated based on the signal intensity ratio of chemical shifts $\delta$= 4.101 ppm and $\delta$= 7.369 ppm (9.26:1.00) in Figure 2. The weight of PCL was 4.655 g, the yield of this reaction was 90.7%.

PCL-CTA was synthesized by a DMAP catalyzed esterification reaction from PCL and a chain transfer agent with a carboxylic acid end group. DCC was used to remove water generated during the reaction. The conjugation of chain transfer agent onto PCL was confirmed by the disappearance of chemical shift signal at $\delta$= 3.667 ppm in Figure 3. The weight of PCL-CTA was 0.386 g, the yield of this reaction was 77.0%.

PCL-*b*-PHPMA was synthesized from a reversible addition−fragmentation chain-transfer (RAFT) polymerization initiated by AIBN. The molecular weight of PCL-*b*-PHPMA was 5.44 kDa and the repeating number *y* was 17 determined by $^1H$ NMR. This was calculated based on the signal intensity ratio of chemical shifts $\delta$= 3.984 ppm and $\delta$= 3.701 ppm in Figure 4. The weight of PCL-*b*-PHPMA was 0.065 g, the yield of this reaction was 13%.

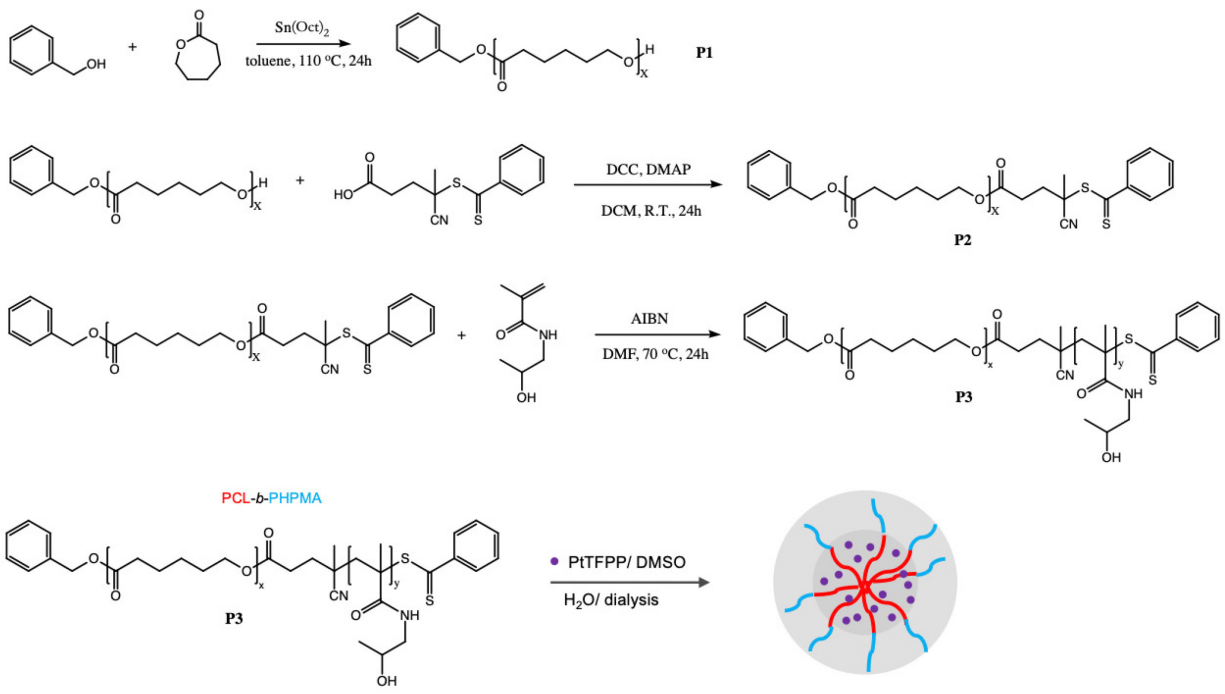


Scheme 1. Synthesis of PCL-*b*-PHPMA and preparation of micelles

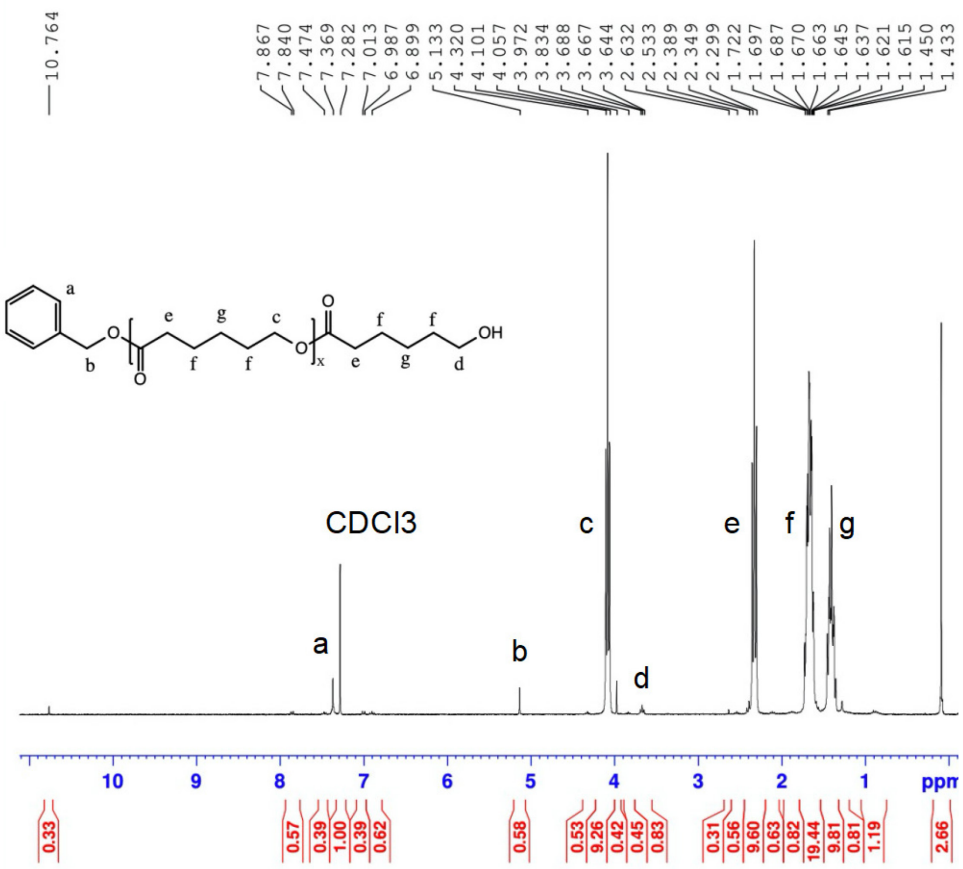


Figure 2. The NMR spectrum of PCL

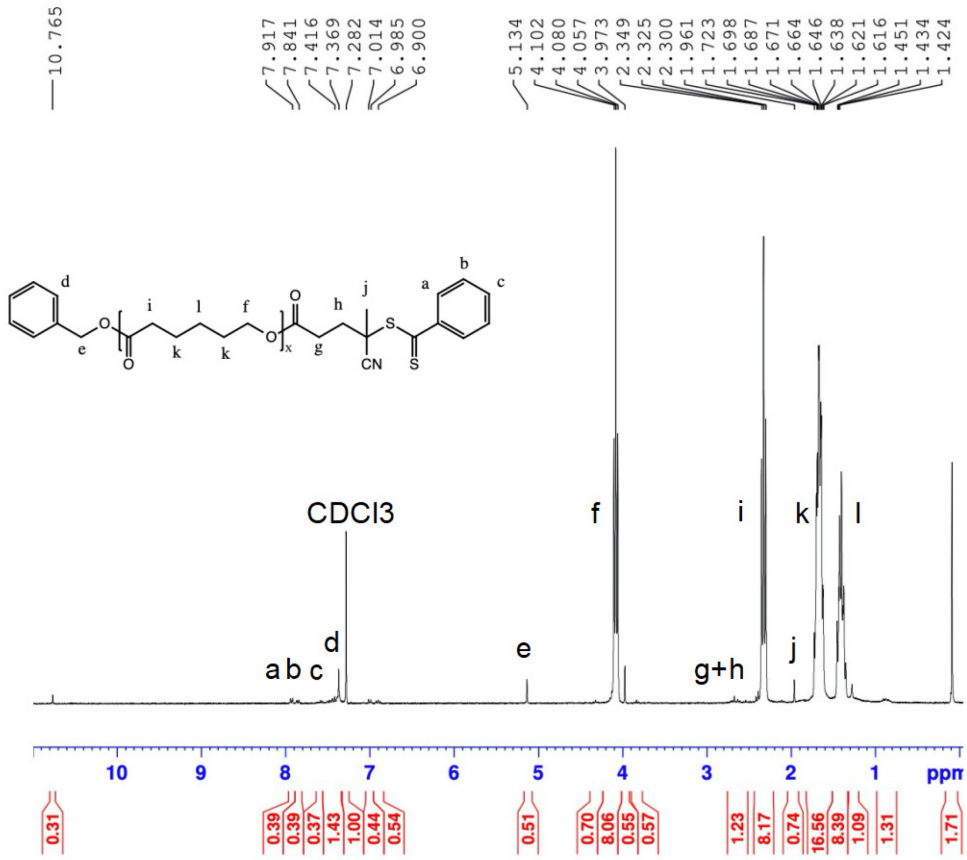


Figure 3. The NMR spectrum of PCL-CTA

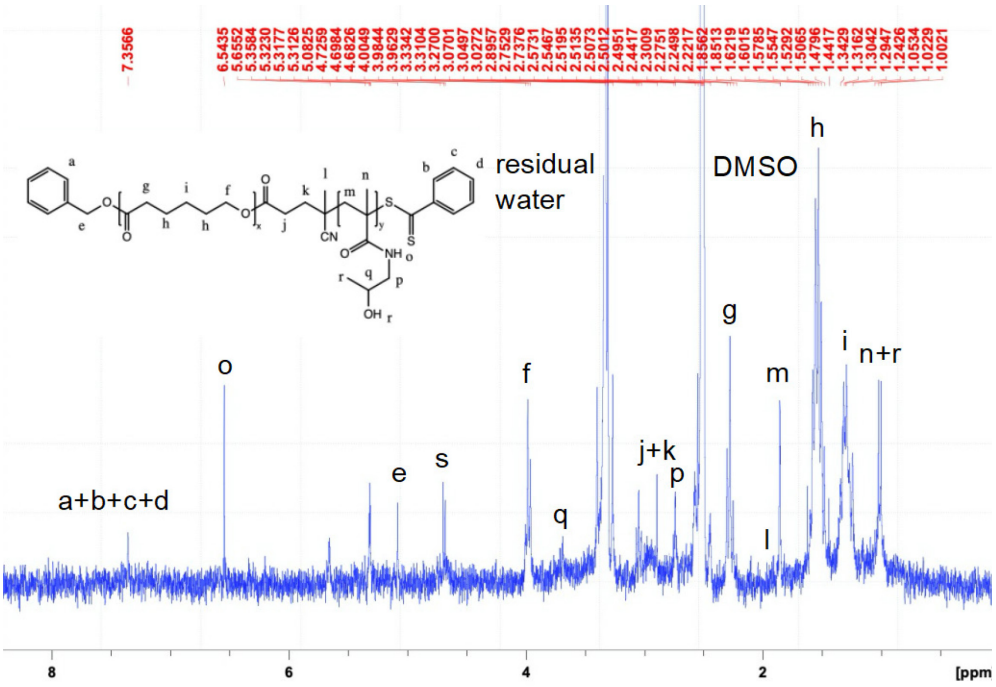


Figure 4. The NMR spectrum of PCL-*b*-PHPMA

## 3.2 Micelles Preparation and Characterization

The average diameter of micelle nanoparticles in aqueous solutions was determined using DLS analysis. We found the average diameter to be 21.43 nm with a polydispersity index (PDI) of 0.301 by DLS at room temperature, as shown in Figure 5.

The concentration of PCL-*b*-PHPMA and PtTFPP incorporated in the micelle solution need to be calibrated for quantification. To calibrate the micelle solutions, 1 mL of micelle solution was lyophilized and the total weight of both PtTFPP and PCL-*b*-PHPMA was 0.8 mg. A standard curve of a series of PtTFPP concentrations was made based on their absorption at 390 nm, as shown in Figure 6.

$$Absorption = 6.776 * [PtTFPP] + 2.085$$

In the equation, [PtTFPP] is the concentration of PtTFPP in solution. The absorption of the lyophilized sample which was re-dissolved in 1 mL of solvent was 2.548 au and thus the concentration of PtTFPP in micelle solutions was 0.068 mg/mL. By eliminating the weight of PtTFPP in the weight of the lyophilized sample, the concentration of PCL-*b*-PHPMA in micelle solution was calculated to be 0.732 mg/mL.

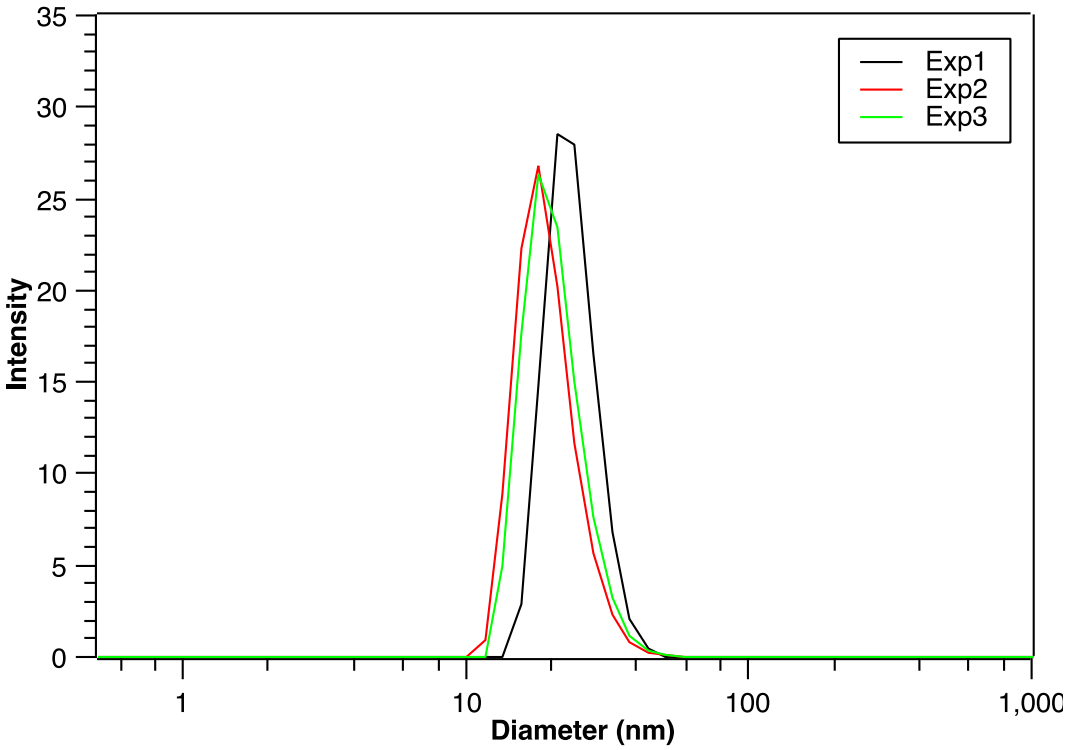


Figure 5. Particle size distributions of micelles measured for three times

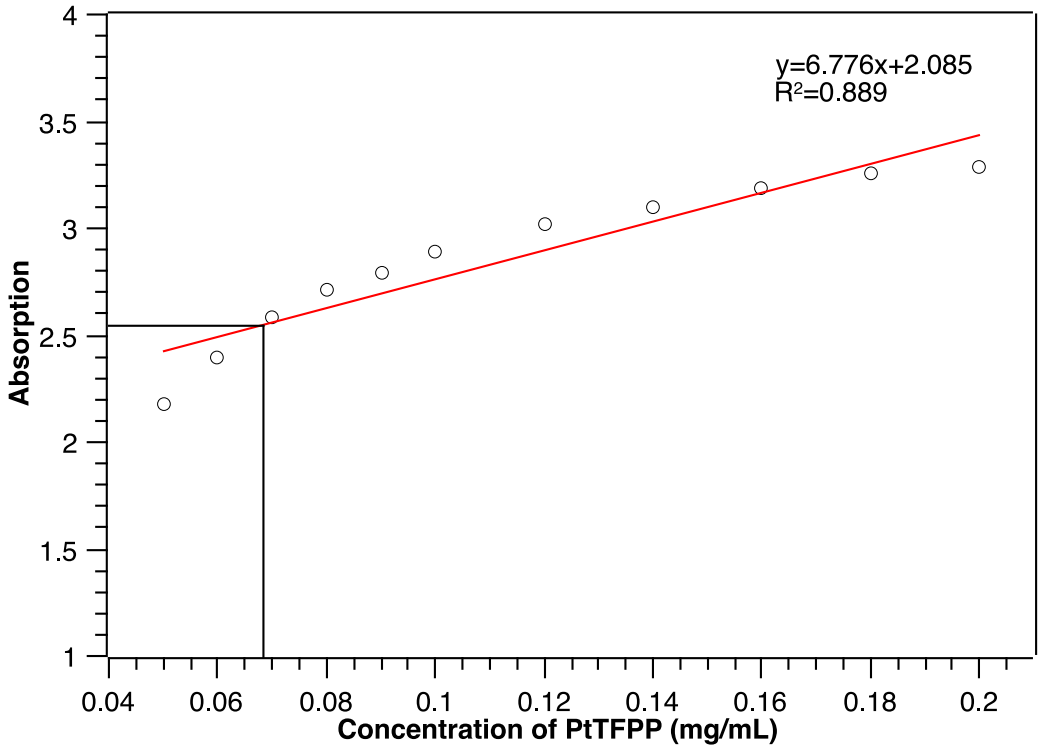


Figure 6. Standard curve of PtTFPP in mixture of DMSO and water (90:10) and corresponding concentration of PtTFPP of the micelle

## 3.3 Oxygen Sensing Abilities in Micelle Solutions

Phosphorescence spectra were measured for both normoxic and hypoxic micelle solutions. For normoxic micelle solutions, the concentration of dissolved oxygen was 8 mg/L. For hypoxic micelle solutions, the dissolved oxygen was completely removed. Strong emission at 650 nm were observed. Based on Figure 7, the peak emission intensity at 650nm decreased by 36.3% (1507.8 au to 960.4 au) when dissolved oxygen concentration increased from 0 to 21%. This was because as more oxygen molecules were present, more quenching occurred and therefore less intense emission could be given by the luminescent molecule PtTFPP.

The oxygen sensing property of the micelle solution indicated successful encapsulation of PtTFPP by amphiphilic block copolymer PCL-*b*-PHPMA. Otherwise, PtTFPP would not be compatible with water solutions and would not show phosphorescence.

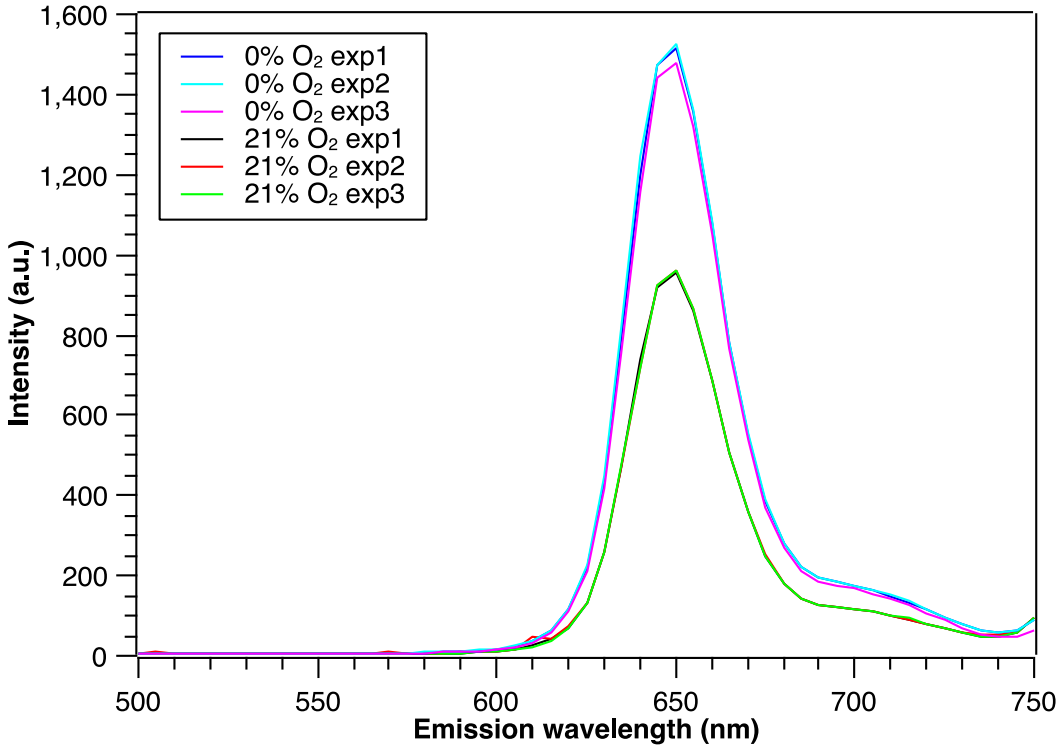


Figure 7. Phosphorescence spectra of oxygen sensors in normoxic solutions and hypoxic solutions under the excitation wavelength of 390 nm at room temperature

## 3.4 Oxygen Sensing Abilities of Sensors in Collagen Hydrogels

Confocal images were taken for oxygen sensors in collagen hydrogels with and without KIA cells consuming oxygen for 24h. The oxygen sensors in both samples were mixed well with the collagen I before gelation and were uniformly dispersed in the hydrogel.

Figure 8 is the confocal image of collagen hydrogel with oxygen sensors embedded only. Without KIA cells consuming oxygen in this sample, the oxygen sensors showed

uniform phosphorescence due to uniformly distributed oxygen level in the collagen hydrogel.

Figure 9 is the confocal image of collagen hydrogel with both KIA cells and oxygen sensors embedded. With KIA cell cluster consuming oxygen shown in Figure 9, the oxygen level inside the cell cluster should be lower than where cells were less dense. This was verified by the confocal image. The signals were stronger inside the cell cluster than the surrounding, indicating a difference in oxygen concentration.

However, when comparing phosphorescence intensity between the two samples, the emission in collagen hydrogels with KIA cells embedded to consume oxygen should be more intense than in collagen hydrogels without KIA cells. This is contradictory to our findings. One explanation could be that the photostability of oxygen sensors was affected by the KIA cells. More future research on photostability of oxygen sensors and their biocompatibility with various cell types are expected to prove this.

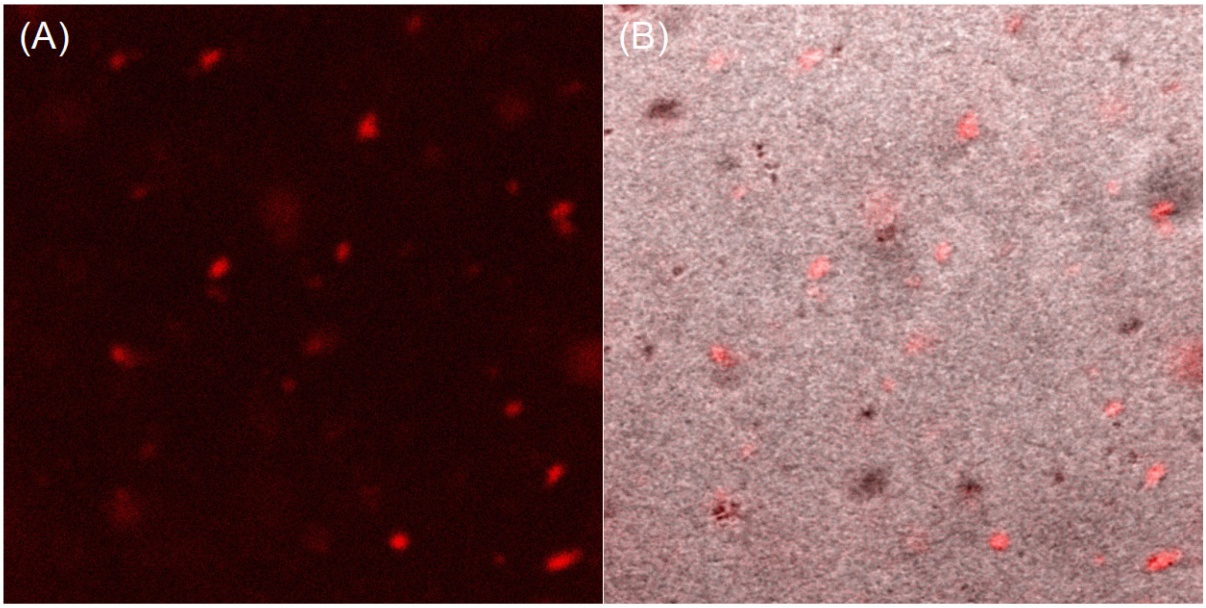


Figure 8. Confocal images of collagen hydrogels with oxygen sensors only embedded for 24h under the excitation wavelength of 405 nm. (A) Red channel; (B) Composite of red channel and bright field.

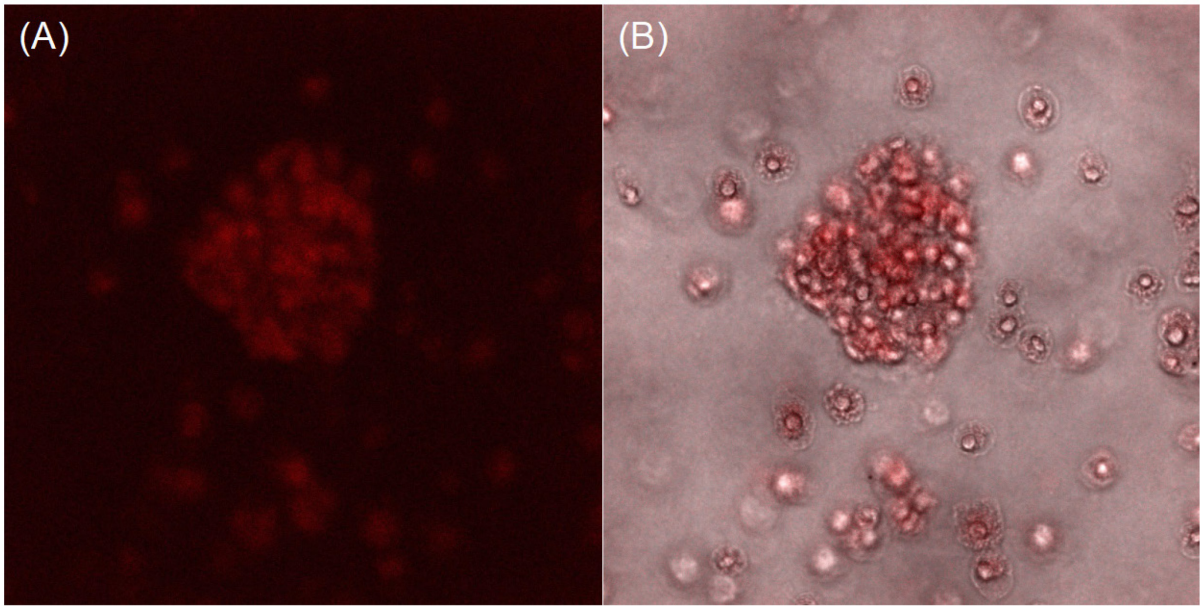


Figure 9. Confocal images of collagen hydrogels with KIA cells and oxygen sensors embedded for 24h under the excitation wavelength of 405 nm. (A) Red channel; (B) Composite of red channel and bright field.

# 4. Conclusion

We have successfully synthesized amphiphilic block copolymers PCL-*b*-PHPMA through a series of polymerization and prepared micelles to incorporate oxygen sensing probe PtTFPP. The micellar oxygen sensors were characterized to be nanoscale and it showed good oxygen sensing ability in micelle solutions. The peak emission intensity at 650 nm decreased by 36.3% when oxygen concentration increased from 0 to 21%. We also embedded oxygen sensors in collagen I hydrogels with and without KIA cells consuming oxygen and confocal images were taken after incubation for 24 h. Stronger phosphorescence were observed where cells gathered, suggesting a lower oxygen concentration inside cell cluster due to KIA cells consuming oxygen. Future research focus on photostability of these oxygen sensors in collagen hydrogels with cells.

# Bibliography


1. Semenza, G.L.. Oxygen Homeostasis. *WIREs Syst Biol Med*. 2010; 2:336-361. https://doi.org/10.1002/wsbm.69.
2. Michael Graham Espey. Role of oxygen gradients in shaping redox relationships between the human intestine and its microbiota. *Free Radical Biology and Medicine*. 2013; 55:130-140. https://doi.org/10.1016/j.freeradbiomed.2012.10.554.
3. Samantha N. Greer, Julie L. Metcalf, Yi Wang, Michael Ohh. *The updated biology of hypoxia- inducible factor. EMBO J*. 2012; 31:2448-2460. https://doi.org/10.1038/emboj.2012.125.
4. Hani Choudhry, Adrian L. Harris. Advances in Hypoxia-Inducible Factor Biology. *Cell Metabolism*. 2018; 27(2):281-298. https://doi.org/10.1016/j.cmet.2017.10.005.
5. Yifeng Zhang, Irini Angelidaki. A simple and rapid method for monitoring dissolved oxygen in water with a submersible microbial fuel cell (SBMFC). *Biosensors and Bioelectronics.* 2012; 38(1):189-194. https://doi.org/10.1016/j.bios.2012.05.032.
6. Skoog A. D, West M. D., Holler J. F., et al. Fundamentals of analytical chemistry. Nelson Education, 2013.
7. Tai H., Yang Y., Liu S., Li D. A Review of Measurement Methods of Dissolved Oxygen in Water. *Computer and Computing Technologies in Agriculture V*. CCTA 2011. IFIP Advances in Information and Communication Technology, vol 369. Springer, Berlin, Heidelberg. https://doi.org/10.1007/978-3-642-27278-3_58.

8. Jiang Z, Yu X, Zhai S, Hao Y. Ratiometric Dissolved Oxygen Sensors Based on Ruthenium Complex Doped with Silver Nanoparticles. *Sensors*. 2017; 17(3):548. https://doi.org/10.3390/s17030548.
9. Wang X, Wolfbeis OS. Optical methods for sensing and imaging oxygen: materials, spectroscopies and applications. *Chemical Society Reviews*. 2014: 43(10):3666-3761. https://doi.org/10.1039/C4CS00039K.
10. Huan Qin, Ting Zhou, Sihua Yang, Da Xing. Fluorescence Quenching Nanoprobes Dedicated to In Vivo Photoacoustic Imaging and High-Efficient Tumor Therapy in Deep-Seated Tissue. *Small*. 2015; 11(22):2675-2686. https://doi.org/10.1002/smll.201403395.
11. Cristina Flors, Michael J Fryer, Jen Waring, Brandon Reeder, Ulrike Bechtold, Philip M Mullineaux, Santi Nonell, Michael T Wilson, Neil R Baker. Imaging the production of singlet oxygen *in vivo* using a new fluorescent sensor, Singlet Oxygen Sensor Green. *Journal of Experimental Botany*. 2006; 57(8):1725–1734. https://doi.org/10.1093/jxb/erj181.
12. Joel Keizer. Nonlinear Fluorescence Quenching and the Origin of Positive Curvature in Stern-Volmer Plots. J. Am. Chem. Soc. 1983; 105:1494-1498.
13. D. Patrick O'Neal, M. Adam Meledeo, Justin R. Davis, Bennett L. Ibey, V. Alexander Gant, Michael V. Pishko, Gerard L. Oxygen Sensor Based on the Fluorescence Quenching of a Ruthenium Complex Immobilized in a Biocompatible Poly(Ethylene Glycol) Hydrogel. IEEE sensors journal. 2004; 4(6):728-734.

14. Su F, Alam R, Mei Q, Tian Y, Youngbull C, et al. (2012) Nanostructured Oxygen Sensor - Using Micelles to Incorporate a Hydrophobic Platinum Porphyrin. *PLoS ONE* 7(3): e33390. https://doi:10.1371/journal.pone.0033390.

15. Cheng-Shane Chu, Che-An Lin. Optical fiber sensor for dual sensing of temperature and oxygen based on PtTFPP/CF embedded in sol–gel matrix. *Sensors and Actuators B: Chemical*. 2014; 195:259-265. https://doi.org/10.1016/j.snb.2014.01.032.

16. Tai-Sheng Yeh, Chen-Shane Chu, Yu-Lung Lo. Highly sensitive optical fiber oxygen sensor using Pt(II) complex embedded in sol–gel matrices. *Sensors and Actuators B: Chemical. 2006*; 119(2):701-707. https://doi.org/10.1016/j.snb.2006.01.051.

17. Ti-Wen Sung, Yu-Lung Lo. Dual sensing of temperature and oxygen using PtTFPP-doped CdSe/SiO2 core–shell nanoparticles. *Sensors and Actuators B: Chemical*. 2012; 173:406-413. https://doi.org/10.1016/j.snb.2012.07.028.

18. Krimmer SG, Pan H, Liu J, Yang J, Kopeček J. Synthesis and characterization of poly(ε-caprolactone)-block-poly[N-(2-hydroxypropyl)methacrylamide] micelles for drug delivery. *Macromol Biosci*. 2011; 11(8):1041-51. doi: 10.1002/mabi.201100019. Epub 2011 May 12. PMID: 21567954; PMCID: PMC4598047.

19. Svetlana Petrova, Damir Klepac, Rafał Konefał, Sami Kereïche, Lubomír Kováčik, Sergey K. Filippov. Synthesis and Solution Properties of PCL-b-PHPMA Diblock Copolymers Containing Stable Nitroxyl Radicals.

*Macromolecules*. 2016; 49(15):5407-5417. https://doi: 10.1021/acs.macromol.6b01187.

20. Xianshao Zou, Tingting Pan, Jiapei Jiang, Gang Li, Cheng Song, Ruofan Sun, Ziyun Yang, Dazhi Sun, Chunhui Hou, Meiwan Chen, Yanqing Tian. Poly(ε-caprolactone)-containing graft copolymers for ratiometric extracellular oxygen sensing. *Sensors and Actuators B: Chemical*. 2017; 108-118. https://doi.org/10.1016/j.snb.2017.03.126.
21. Wolff P, Heimann L, Liebsch G, Meier RJ, Gutbrod M, van Griensven M, Balmayor ER. Oxygen-distribution within 3-D collagen I hydrogels for bone tissue engineering. *Mater Sci Eng C Mater Biol Appl*. 2019; 95:422-427. https://doi: 10.1016/j.msec.2018.02.015. Epub 2018 Feb 21. PMID: 30573266.
22. Yuan, T, Zhang, L, Li, K, Fan, H, Fan, Y, Liang, J, Zhang, X. Collagen hydrogel as an immunomodulatory scaffold in cartilage tissue engineering. J Biomed Mater Res Part B. 2014; 102B: 337– 344. https://doi.org/10.1002/jbm.b.33011.